TiO_2 Surface Functionalization to Control the Density of States

Amanda J. Morris and Gerald J. Meyer*

Departments of Chemistry and Materials Science and Engineering, Johns Hopkins University, 3400 North Charles Street, Baltimore, Maryland 21218

Received: February 14, 2008; Revised Manuscript Received: August 1, 2008

Surface functionalization of mesoporous nanocrystalline (anatase) TiO_2 thin films with decyltriethoxysilane, octyltriethoxylsilane, hexyltriethoxysilane, decylphosphonic acid, undecanoic acid, and hemin was accomplished by room temperature reactions in toluene, acetonitrile, or DMSO. Surface functionalization was verified by attenuated total reflection infrared spectroscopy (ATR-FTIR) and the integrated density of unfilled TiO_2 states (DOS) were probed by spectroelectrochemical, reactivity, and excited-state injection yield measurements. With the exception of hexyltriethoxysilane, all surface functionalizations were found to shift the DOS positive on an electrochemical scale (away from the vacuum level) in 0.1 M tetrabutylammonium ion containing electrolyte. The magnitude of the effect was found to be dependent on the surface coverage. The potential onset of the unfilled TiO_2 states was not affected by functionalization in 0.1 M lithium ion containing electrolyte but the DOS at more negative potentials was significantly decreased. The 532 nm sensitized injection yield with $Ru(dcb)(bpy)_2(PF_6)$, where dcb is 4,4′-$(COOH)_2$-2,2′-bipyridine and bpy is bipyridine, was 0.89 ± 0.09 for all surface functionalizations. An enhancement of the open circuit photovoltage in regenerative solar cells with 0.5 M LiI/0.05 M I_2 was measured after surface functionalization, and an analysis of this data with the diode equation indicated decreased rates for I_3^- reduction by factors of 7−330. The second-order rate constant for the reduction of carbon tetrachloride by electrochemically reduced TiO_2 that had been surface functionalized with decytriethoxysilane, 0.21 ± 0.01 M^{-1} s^{-1}, was decreased relative to an unfunctionalized TiO_2 thin film, 1.02 ± 0.03 M^{-1} s^{-1}, behavior attributed to the ability of the functionalized surface to prevent close encounters with electron acceptors.

Introduction

Adsorption of ions or molecules to the surface of a semiconductor is known to induce a change in the flat band potential.[1] Since the doping level and band gap are usually insensitive to surface adsorption, the energetic positions of the conduction and valence bands shift in parallel relative to a reference potential. Perhaps the most well-known example of this is proton adsorption−desorption equilibrium at aqueous metal oxide interfaces that gives rise to a Nernstian shift (59 mV/pH unit) of the band edge positions.[2] There are in fact many other examples.[3] Adsorption-induced shifts in semiconductor energy levels are sometimes undesirable and can lead to poor open circuit photovoltages in solar cells or low quantum yields in photocatalysis, for example.[4−14] In addition, data interpretation is often complicated by fluxuations in the adsorbate concentration that occur during the course of fundamental experiments. Therefore, a method by which flat band potentials could be tuned and then fixed at an optimal energy level would be of significant utility. One method by which this might be achieved is through reaction and binding of molecular compounds with the semiconductor surface, referred to here as surface functionalization. The functionalization of semiconductor surfaces has indeed been a focus of experimental research for several decades.[4−14]

Adsorption-induced shifts in the band edges are expected to be significant for the high surface area mesoporous nanocrystalline (anatase) TiO_2 semiconductor thin films utilized in dye sensitized solar cells. Grätzel reported an open circuit voltage enhancement of 280 mV, corresponding to an 8.5% global conversion efficiency, after functionalization of mesoporous nanocrystalline (anatase) TiO_2 with 4-*tert*-butylpyridine (TBP).[4] In this work, and also in later studies by Arakawa, a negative shift in dark current onset for I_3^- reduction was observed with TBP, indicative of attenuation of tri-iodide reduction.[4,5] Even larger cathodic shift of 700 mV was reported after functionalization of TiO_2 by poly(methylsiloxane).[6] The enhanced open circuit voltages and decreased dark currents do not necessarily result from shifts in the flat band potential and may simply result from a "blocking layer" at the TiO_2 surface that inhibits close encounters of I_3^-. To this end, Grätzel and colleagues determined the effect of guanidinobutyric acid (GBA) on the flat band potential of sensitized TiO_2 by cyclic voltammetry in 1-propyl-3-methylimidazolium-containing ionic liquid.[14] A 50 mV negative shift of the flat band potential was measured relative to an unfunctionalized material.

A remarkable cation-dependent shift in the flat band potential of TiO_2 has also been reported with Li^+ adsorption in nonaqueous solution. In Li^+-containing acetonitrile electrolyte the flat band potential shifts to −0.9 V vs SCE compared to −2.0 V vs SCE in tetrabutylammonium nitrile (TBA^+)-containing electrolyte.[15] The effect was not limited to Li^+ but has been observed for other alkali and alkaline earth cations of magnitude dependent on the cation size-to-charge ratio.[16]

A significant challenge with mesoporous nanocrystalline thin films is to quantify a flat band potential under *any* experimental conditions. The small size of the semiconductor particle precludes the standard analysis of capacitance data that is commonly employed for planar semiconductor materials.[3] As was previously mentioned, open-circuit photovoltage or the dark current changes measured after surface functionalization may

* E-mail: meyer@jhu.edu.

10.1021/jp801338y CCC: $40.75
Published on Web 10/29/2008

have kinetic and/or thermodynamic origins. The most commonly cited flat band potentials for nanocrystalline TiO_2 thin films were determined from spectoelectrochemical measurements with an accumulation layer model.[15] This model assumes the presence of a sharp conduction band edge whose potential does not change as the Fermi energy is raised. Neither of these assumptions has been validated and there is now compelling evidence that a broad distribution of acceptor states are present in nanocrystalline TiO_2. Bisquert has recently reported a more comprehensive model for the potential distribution of nanocrystalline TiO_2 thin films that indicates an exponential tailing of band states beneath a formal conduction band.[17] To our knowledge, a Bisquert-type analysis has not been previously applied to spectroelectrochemical data of surface functionalized TiO_2.

The goal of this manuscript was to provide a definitive answer to whether surface functionalization shifts the semiconductor flat band potential, acts as a blocking layer, or both. We were specifically interested in how surface functionalization might prevent or facilitate shifts in the density of acceptor states that are known for potential determining cations such as Li^+. Comparative studies with long chain siloxanes, carboxylic acids, and phosphonic acids as well as a redox active heme were performed. For the first time, the direct reduction of acceptors by $TiO_2(e^-)$ was measured spectroscopically to more firmly establish the origin of changed in the V_{oc}. The results show directly that back electron transfer is inhibited by surface functionalization. They also unequivocally illustrate that flat band potential shifts are dominated by cation adsorption in acetonitrile that can be controlled by surface functionalization. Significantly, the data is inconsistent with the sharp conduction band edge implied by the accumulation layer model. Instead, a broad distribution of acceptor states was observed and quantified under experimentally meaningful conditions.

Experimental Section

Materials. Dimethyl sulfoxide (DMSO) >99.9% (Fisher Scientific), acetonitrile (ACN) >99.9% (Burdick and Jackson), titanium(IV) isopropoxide 97% (Aldrich), methanol (MeOH) >99.9% (Aldrich), carbon tetrachloride >99.9% (Aldrich), tetrabutylammonium hydroxide 40% (Fluka), potassium hydroxide ACS grade (Fisher), decyltriethoxysilane (Gelest), octyltriethoxysilane (Gelest), hexyltriethoxysilane (Gelest), *n*-decylphosphonic acid 99% (Strem), undecanoic acid 99% (Aldrich), iron(III) protoporphyrin chloride (hemin) >98% (Fluka), tetrabutylammonium (TBA^+) perchlorate >99.9% (Fluka), tetrabutylammonium hexafluorophosphate >99.9% (Fluka), and lithium perchlorate >99.99% (Aldrich), lithium iodide 99.9% (Aldrich), and iodine 99.8% (Aldrich) were used as received. $Ru(dcb)(bpy)_2(PF_6)_2$ was synthesized according to a previously reported procedure.[16]

Materials Preparation. ***Nanocrystalline TiO_2.*** Transparent TiO_2 nanocrystals (anatase ~15 nm diameter) were prepared by hydrolysis of $Ti(iOPr)_4$ using a sol−gel technique previously described in the literature.[18] The TiO_2 nanocrystals were cast as mesoporous thin (~10 μm) films onto microscope glass slides for spectroscopic measurements or fluorine-doped tin oxide (FTO) for electrochemical measurements. In both cases, the thin films were heated at 420 °C for 30 min.

Surface Functionalization. Freshly prepared TiO_2 films were base treated in pH 11 potassium hydroxide solutions for 2 min and then functionalized by the overnight room temperature reactions described below. Hemin/TiO_2 was prepared by reaction of 2−8 μM hemin in DMSO. Silane/TiO_2 films were prepared by reactions with 500 mM solutions of the appropriate triethoxysilane in toluene. Decylphosphonic acid/TiO_2 films were prepared by reactions of 100 mM n-decylphosphonic acid and 200 mM tetrabutylammonium hydroxide in acetonitrile. Undecanoic acid/TiO_2 films were prepared by reactions of 500 mM undecanoic acid and 500 mM tetrabutylammonium hydroxide in acetonitrile. The functionalized materials were rinsed under a gentle flow of acetonitrile (or DMSO for hemin/TiO_2) for about 10 s prior to electrochemical or spectroscopic characterization.

In some cases, the functionalized TiO_2 was sensitized to visible light by overnight reactions at room temperature with a $Ru(dcb)(bpy)_2(PF_6)$ solution in acetonitrile.

Spectroscopic Measurements. ***FTIR-ATR.*** Attenuated total reflectance (ATR) infrared spectra were obtained with a Golden Gate Reflectance diamond cell in a Nexus 670 Thermo-Nicolet FTIR spectrometer. The samples were rinsed with acetonitrile and dried before collecting spectral data. The data shown is an average of 32 scans with 2 cm^{-1} resolution and was recorded under a N_2 atmosphere. The spectral data was not corrected for nonzero baselines or the wavelength dependent penetration depth of the light.

Electronic Spectroscopy. Steady-state UV−vis and long timescale transient UV−vis spectroscopy was carried a Varian Cary 50 spectrometer.

Transient Absorption Spectroscopy. The quantum yields for excited-state electron injection into TiO_2 were quantified by comparative actinometry measurements on a nanosecond time scale as previously described.[19] A $[Ru(bpy)_3](PF_6)_2$ doped poly(methyl methacrylate) (PMMA) thin film, whose optical absorption and physical dimensions were very similar to the sensitized TiO_2 films, was used as the actinometer. The absorbance of the actinometer and a $Ru(dcb)(bpy)_2^{2+}/TiO_2$ sensitized film were approximately matched at the excitation wavelength. A literature value of $(-1.00 \pm 0.09) \times 10^4$ M^{-1} cm^{-1} at 450 nm for the difference between the extinction coefficients of the excited-state and ground-state actinometer was used.[19] The $Ru(dcb)(bpy)_2^{2+}$ surface coverage was maintained between 1.38 and 2.20 $\times$ 10^{-8} mol/cm^2. Nanosecond transient absorption measurements were performed with an apparatus that has been previously described except the 532 nm excitation source used here was from a Quantel Brilliant B Nd:YAG laser.[19]

Spectro-electrochemistry. A standard three-electrode arrangement with a TiO_2 film deposited on FTO glass as the working electrode, a Pt disk counter electrode, and Ag/AgCl as the reference electrode was assembled in a custom quartz cuvette. All potentials reported are vs the Ag/AgCl electrode unless otherwise noted. Ferrocene measured in a 100 mM $TBAClO_4$ acetonitrile electrolyte was used as a reference electrode calibration standard, $E_{1/2}(FeCp_2^{+/0}) = 376$ mV. The cuvette was placed in a Varian Cary 50 spectrophotometer and the potential was controlled with a BAS CV-50W potentiostat. The 100 mM electrolyte acetonitrile or methanol solutions were purged with Ar prior to measurements. In a typical experiment, the potential was stepped 100 mV and the absorption spectrum was recorded. Each potential was held until at least 90% of the steady state absorbance at 800 nm was reached which typically took less than 100 s. The potential range was kept between −400 and −800 mV as significant desorption of both undecanoic acid and decylphosphonic acid were observed at more negative potentials.

CCl_4 Reduction. A functionalized TiO_2 thin film was placed in Ar-saturated MeOH and was illuminated with band gap excitation (>320 nm) from a 150 W xenon arc lamp for 3 min

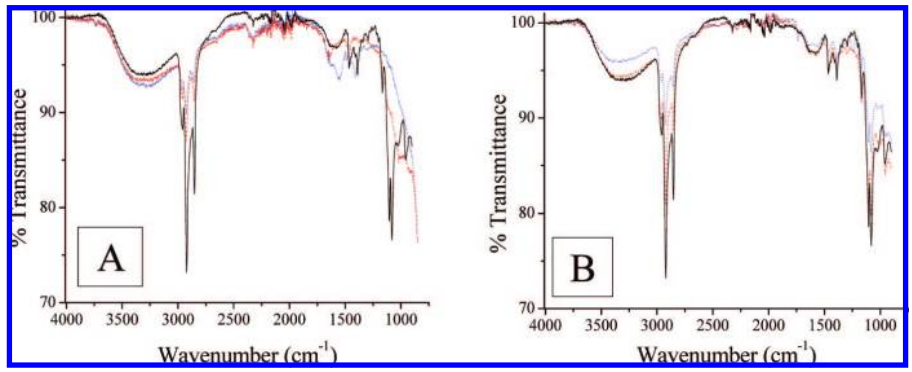

Figure 1. ATR-FTIR of nanocrystalline TiO_2 thin films functionalized with (A) triethoxydecylsilane/TiO_2 (−), decylphosphonic acid/TiO_2 (− − −), and undecanoic acid/TiO_2 (• • •), and (B) a series of long chain silanes decyltriethoxysilane/TiO_2 (−), octyltriethoxysilane/TiO_2 (− − −), and hexyltriethoxysilane/TiO_2 (• • •).

during which time the characteristic color of $TiO_2(e^-)$ was apparent. The sample was then removed from the light and reactions with CCl_4 were carried out in the dark in a Varian Carey 50 spectrometer. After 1 minute of data collection an aliquot of a 0.1 M CCl_4/MeOH solution was added to the sample and the absorption change at 800 nm was monitored. The absorption change was found to be exponential and the resulting data was analyzed by the following equation:

$$k_{obs} = k_o + k_{red}[CCl4] \quad (2)$$

Here k_o was the rate constant for background reductions in the absence of the CCl_4 acceptor and k_{red} is the second-order rate constant. Under all condition reported herein, $k_{red}[CCl_4] \gg k_o$, such that background contributions to the observed rate constant were not significant.

Photoelectrochemistry. ***Open Circuit Voltage.*** Photoelectrochemical measurements of $Ru(dcb)(bpy)_2^{2+}$ sensitized TiO_2 thin films were made in a custom fabricated two-electrode Teflon cell at room temperature. The sensitized films were functionalized with decyltriethoxysilane, octyltriethoxylsilane, hexyltriethoxysilane, decylphosphonic acid, or undecanoic acid. The $Ru(dcb)(bpy)_2^{2+}$ surface coverage was between 1.38 and 1.54 $\times 10^{-8}$ mol/cm^2. A 0.283 cm^2 surface area was illuminated in a 0.5 M LiI/0.05 M I_2 acetonitrile solution containing a Pt mesh counter electrode. Illumination was done through the FTO side of the slide using either a PhotoMax 100 W Xe lamp coupled to a 1/4 m Oriel Cornerstone monochromator with 425 nm light or the 488 nm line of a Coherent Ar^+ laser. Incident irradiance was measured using a Graseby Optronics S370 optometer with a silicon UDT detector. Minor differences in the surface coverages were corrected for by varying the incident irradiance with neutral density filters. The voltages were measured using a Keithley 617 electrometer before and after 3 min of illumination.

Results

Surface functionalization of mesoporous nanocrystalline TiO_2 thin films with decyltriethoxysilane, octyltriethoxylsilane, hexyltriethoxysilane, decylphosphonic acid, and undecanoic acid was accomplished by room temperature reactions in acetonitrile or toluene. The functionalized films were characterized by attenuated total reflectance FTIR (ATR-FTIR). Figure 1 shows ATR-FTIR spectra obtained after reaction of decyltriethoxysilane, octyltriethoxylsilane, hexyltriethoxysilane, decylphosphonic acid, and undecanoic acid with the nanocrystalline TiO_2 thin film. The spectra showed features in the range of 2800−3000 cm^{-1} that are assigned to the asymmetric and symmetric stretching of the $-CH_2$ groups on the carbon chain. Absorptions specific to the surface binding group were also observed. Assignments based on literature values are tabulated in the Supporting Information.[13,20−24] The spectra also showed a broadband centered at 3400 cm^{-1} and a band at 1630 cm^{-1} due to adsorbed water.

Reduction of the TiO_2 thin films in a standard electrochemical cell resulted in a characteristic visible−near IR absorption attributed to TiO_2 electrons, $TiO_2(e^-)$s.[15] The absorption spectra were found to be insensitive to surface functionalization (except hemin/TiO_2) and the normalized spectra were independent of the applied potential over the range studies, −400 to −800 mV vs Ag/AgCl. In all cases, the absorption at 800 nm was directly proportional to the moles of $TiO_2(e^-)$s per cm^2, Γ, eq 3,

$$\Gamma(\text{mol/cm}^2) = \frac{\text{Absorbance}}{\varepsilon(\text{M}^{-1}\text{cm}^{-1}) \times 1000(\text{cm}^3/\text{L})} \quad (3)$$

where ε is the molar extinction coefficient 1300 M^{-1} cm^{-1} at 800 nm.

Shown in Figure 2 are the results of comparative spectroelectrochemical measurements of the TiO_2 thin films in 100 mM tetrabutylammonium perchlorate acetonitrile electrolyte. In all cases studied, surface functionalization resulted in the appearance of $TiO_2(e^-)$s at equal or more positive potentials than an unfunctionalized TiO_2 thin film. Analysis of the data measured at −800 mV clearly shows that all surface functionalization except hexyltriethoxysilane increased the $TiO_2(e^-)$ concentration relative to unfunctionalized TiO_2. For equal chain length hydrocarbons, the magnitude of the effect was dependent on the surface-binding group: carboxylate < siloxane < phosphonate, Figure 3A. As the chain length of the siloxane increased from hexyl (6), to octyl (8), to decyl (10) so too did the $TiO_2(e^-)$ concentration.

In $LiClO_4$ electrolyte, reduction of surface functionalized films required more negative potentials than did an unfunctionalized TiO_2 thin film, Figure 3. The potential dependent $TiO_2(e^-)$ concentration was sensitive to surface functionalization and increased in the order siloxane < carboxylate < phosphonate, Figure 3A. The influence of the siloxane carbon chain length was small and not well resolved, Figure 3B.

Reduction of a hemin/TiO_2 thin films resulted first in the conversion of hemin to heme, i.e., $Fe^{III} \rightarrow Fe^{II}$, and then the generation of $TiO_2(e^-)$s Figure 4A. Four sharp isosbestic points accompanied the reduction of hemin to heme with a Soret band shift from 398 to 417 nm. The reduction of hemin was complete by −600 mV and a more negative applied bias resulted in the appearance of $TiO_2(e^-)$s. Spectroelectrochemical measurements were conducted with five films that varied in hemin surface

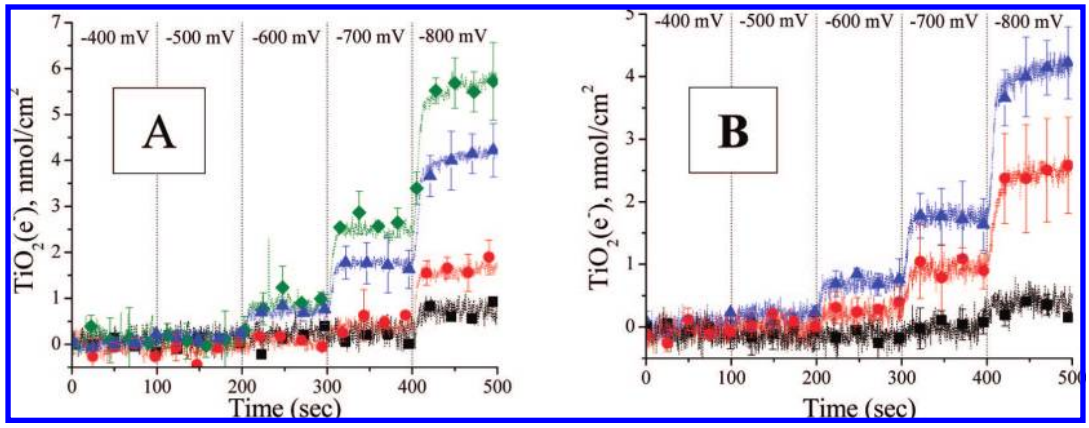

Figure 2. $TiO_2(e^-)$ concentration as a function of applied potential over time in 0.1 M tetrabutylammonium perchlorate acetonitrile electrolyte for (A) undecanoic acid/TiO_2 (• ● •), decyltriethoxysilane/TiO_2 (• ▲ •), decylphosphonic acid/TiO_2 (• ♦ •), and an unfunctionalized TiO_2 film (• □ •); and (B) hexyltriethoxysilane/TiO_2 (• □ •), octyltriethoxysilane/TiO_2 (• ● •), and decyltriethoxysilane/TiO_2 (• ▲ •). Error bars indicate two times the standard deviation calculated from an average of three separate measurements.

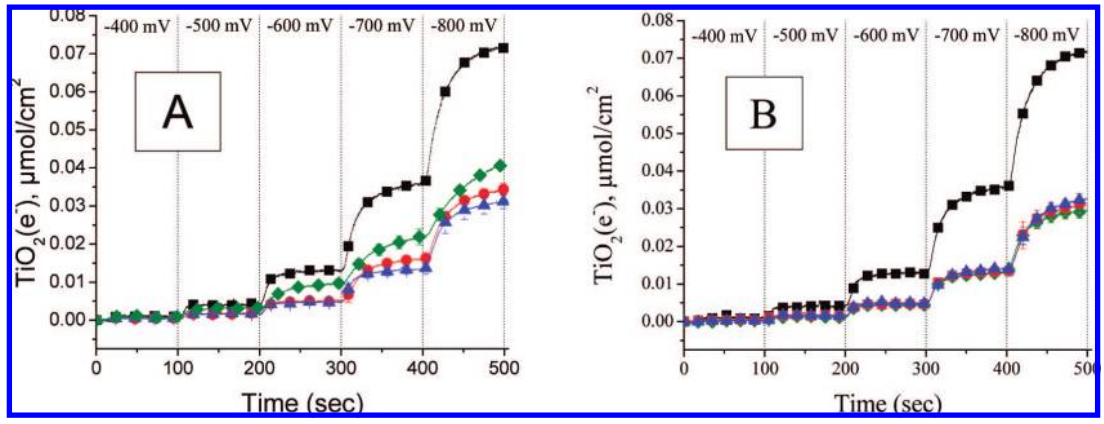

Figure 3. $TiO_2(e^-)$ concentration as a function of applied potential over time in 0.1 M lithium perchlorate acetonitrile electrolyte for (A) undecanoic acid/TiO_2 (• ● •), decyltriethoxysilane/TiO_2 (• ▲ •), decylphosphonic acid/TiO_2 (• ♦ •), and an unfunctionalized TiO_2 film (• □ •); and **(B)** decyltriethoxysilane/TiO_2 (• ● •), octyltriethoxysilane/TiO_2 (• ▲ •), and hexyltriethoxysilane/TiO_2 (• ♦ •), and an unfunctionalized TiO_2 film (• □ •). Error bars indicate two times the standard deviation calculated from an average of three separate measurements.

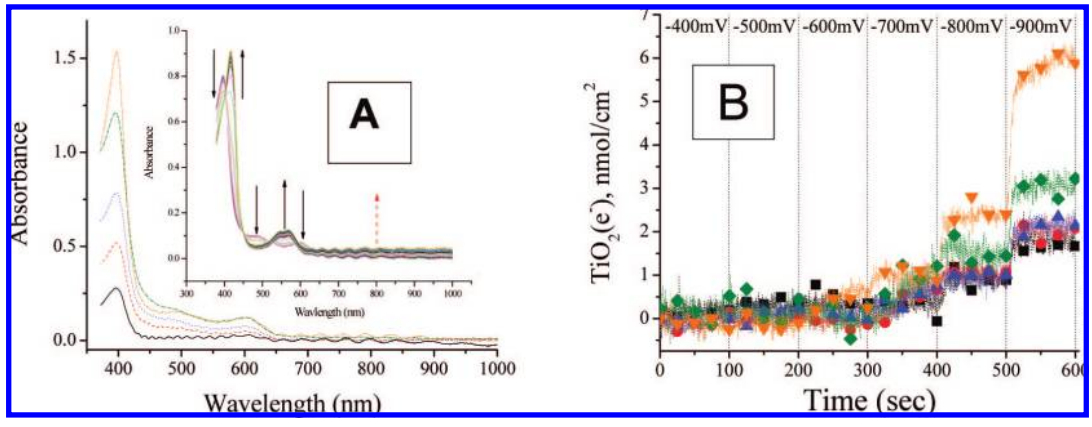

Figure 4. (A) Absorbance spectra of TiO_2 thin films functionalized with different surface coverages of hemin [1.79×10^{-9} (−), 3.63×10^{-9} (− − −), 5.51×10^{-9} (• • •), 8.35×10^{-9} (− • −), and 1.03×10^{-8} mol/cm^2 (• • − • •)]. Inset shows spectral changes as a function of applied negative potential. First hemin (Fe^{III}) was reduced to heme (Fe^{II}) (black arrows) followed by an increase in the $TiO_2(e^-)$ concentration (red dash arrow). (B) The $TiO_2(e^-)$ concentration as a function of applied potential over time in 0.1 M tetrabutylammonium perchlorate acetonitrile electrolyte of TiO_2 films functionalized with different surface coverages of hemin [1.79×10^{-9} (• □ •), 3.63×10^{-9} (• • •), 5.51×10^{-9} (• ▲ •), 8.35×10^{-9} (• ♦ •), and 1.03×10^{-8} mol/cm^2 (• ▲ •)].

coverage from 1.79 to 10.3×10^{-9} mol/cm^2, Figure 4B. Data measured at −900 mV shows a higher $TiO_2(e^-)$ concentration with increased hemin surface coverage.

The sensitized injection quantum yields, ϕ_{inj}, for functionalized $Ru(dcb)(bpy)_2^{2+}/TiO_2$ thin films in 100 mM $LiClO_4$ acetonitrile solution were measured by comparative actinometry

TABLE 1: Quantum Yields for Sensitized Injection, ϕ_{inj}, and Open Circuit Photovoltage Measurements of Functionalized TiO_2 Film in CH_3CN

functionalization	V_{oc}[a] (mV)	relative rate[b]	ϕ_{inj}[c]
unfunctionalized	85	1	0.57 ± 0.12
hexyltriethoxysilane	114	3.2×10^{-1}	0.80 ± 0.06
octyltriethoxysilane	135	1.4×10^{-1}	0.85 ± 0.04
decyltriethoxysilane	229	3.6×10^{-3}	0.93 ± 0.07
decylphosphonic acid	175	3.0×10^{-3}	–
undecanoic acid	125	2.1×10^{-1}	0.97 ± 0.06

[a] The open circuit photovoltage measured in 0.5 M LiI/0.05 M I_2 CH_3CN with 270 $\mu W/cm^2$ of 425 nm light. [b] The rate calculated for I_3^- reduction based on eq 4 relative to an unfunctionalized film. [c] Excited state injection quantum yield, ϕ_{inj}, after 532 nm light excitation of $Ru(dcb)(bpy)_2/TiO_2$ in $LiClO_4 \cdot CH_3CN$.

with 532 nm light.[19] The quantum yields were all close to unity, undecanoic acid had a slightly larger quantum yield compared to decyltriethoxysilane. Triethoxysilane functionalization resulted in quantum yields within 0.82 ± 0.07 regardless of the alkyl chain length, Table 1. Attempts to measure ϕ_{inj} for decylphosphonic acid functionalized films were unsuccessful due to sensitizer desorption in 100 mM $LiClO_4$ acetonitrile solution.

Figure 5 shows the current−voltage curves of functionalized films in 0.5 M LiI/0.05 M I_2 electrolyte solutions. Surface functionalization results in a negative shift of the onset potential for iodide reduction relative to an unfunctionalized TiO_2 film except for undecanoic acid/TiO_2 that showed no measurable change. Decylphosphonic acid shifts the onset potential negative but not as effectively as the decyltriethoxysilane. The behavior with tetrabutylammonium cations was qualitatively similar but the current was about a factor of 2 lower.

The reactivity of $TiO_2(e^-)$s with carbon tetrachloride was quantified spectroscopically. Figure 6 shows the $[TiO_2(e^-)]$ loss in the presence of CCl_4 on a decyltriethoxysilane functionalized film and an unfunctionalized film. The absorption changes were found to be exponential. The inset shows the concentration dependence of the observed rate constants from which second-order rate constants were abstracted, decyltriethoxysilane/TiO_2 ($k_{red} = 0.21 \pm 0.01$ M^{-1} s^{-1}), and TiO_2 ($k_{red} = 1.02 \pm 0.03$ M^{-1} s^{-1}).

The open circuit photovoltage, V_{oc}, was measured for $Ru(dcb)(bpy)_2^{2+}/TiO_2$ films functionalized with decyltriethoxysilane, octyltriethoxylsilane, hexyltriethoxysilane, decylphosphonic acid, or undecanoic acid in 0.5 M LiI/0.05 M I_2 acetonitrile electrolyte with 425 nm light, Table 1. In all cases surface functionalization resulted in an increase in V_{oc} compared to an unfunctionalized $Ru(dcb)(bpy)_2^{2+}/TiO_2$ film, where decyltriethoxysilane/$Ru(dcb)(bpy)_2^{2+}/TiO_2$ resulted in the largest increase in V_{oc}, 144 mV. With 488 nm light the enhancement with surface functionalization of decyltriethoxysilane, decylphosphonic acid, and undecanoic acid was observed over 3 orders of magnitude in irradiance with slopes of ~190 mV/decade, indicative of a nonideality factor of over 3.

Discussion

The surface functionalization of TiO_2 and related metal oxides by molecules with carboxylic acid, phosphonate, or alkoxysilane groups is well documented in the literature.[13,21,25−27] However, the influence of surface functionalization on TiO_2 reactivity and the density of states in nitrile solvents remains much less well understood. Below we discuss this aspect of our results with reference to the relevant published literature.

Density of States. A wide variety of colorless, redox active compounds give rise to intense visible absorption when anchored to anatase TiO_2.[28] The absorption has been assigned to transitions from the compound to the semiconductor and therefore reports on the density of acceptor states in the functionalized TiO_2. Of particular relevance to this work is the report that pyrocatechol functionalization of TiO_2 shifted electronic states from within the forbidden energy gap into the conduction band. The magnitude of the shift was found to be significant, approximately 700 meV, and was inferred from the time response of the $TiO_2(e^-)$ absorption after a negative potential step in aqueous electrolyte.[29] In other studies, the reduction potential of a surface bound compound was measured along with the absorption spectrum and this indicated a Ti^{IV} acceptor state that was well above the expected energetic position of the conduction band edge.[28]

The behavior of nanocrystalline (anatase) TiO_2 thin film electrodes at negative potentials (i.e., forward bias) has been the subject of several studies. Reduction of TiO_2 results in the appearance of a blue-black color that has been attributed to $TiO_2(e^-)$s. Rothenberg and co-workers proposed that an accumulation layer was formed at the semiconductor interface under such conditions and this model has been used to determine flat band potentials under many experimental conditions.[30] A key assumption in this model is that the band edges remain fixed as the Fermi energy is raised toward the vacuum level. If the band edges unpin, significant uncertainty in the flat band potentials would result.[31]

In nanocrystalline semiconductors, the distinction between electronic states in the conduction band from those within the forbidden energy gap can be difficult to establish experimentally. In these studies in acetonitrile or methanol electrolytes, the absorption spectrum of the electrochemically or photochemically reduced TiO_2 was found to be independent of the extent of reduction, electrolyte, or surface functionalization. Therefore, applying Occam's razor we did not attempt to differentiate trapped from conduction band electrons and simply refer to them collectively as $TiO_2(e^-)$s. Our spectral data agree with the literature and the extinction coefficient enables one to quantify the $TiO_2(e^-)$ concentration and hence the Faradaic charge within the film.[32] If it is reasonable to assume that the electrochemical creation of $TiO_2(e^-)$s (and subsequent oxidation) does not influence the energetics of other electronic states in the material, the potential dependent spectral data provides a mapping of the integrated semiconductor density of unfilled states (DOS). We note that this approach is very similar to that of Bisquert and co-workers who analyzed total charge and that of Kay and others who have analyzed voltammetric data in a similar manner.[17,33]

Figure 7 shows a DOS analysis of the spectroelectrochemical data for unfunctionalized TiO_2 and decyltriethoxysilane/TiO_2 in acetonitrile electrolytes. With tetrabutylammonium containing electrolytes, the DOS was shifted about 150 mV positive by decyltriethoxysilane functionalization. Indeed at all potentials where the $TiO_2(e^-)$ concentration could be quantified spectroscopically, the DOS was significantly larger for functionalized TiO_2 relative to the unfunctionalized material except for hexyltriethoxysilane/TiO_2 which showed no measurable effect. For example, at −800 mV the DOS was about 7 times larger for decyltriethoxysilane/TiO_2 relative to unfunctionalized TiO_2. Studies with heme/TiO_2 clearly showed that the magnitude of the effect was directly proportional to the surface concentration. Since heme has two carboxylic acid groups, one might have anticipated a priori that binding would shift the DOS positive on an electrochemical scale like the influence of Bronsted acids

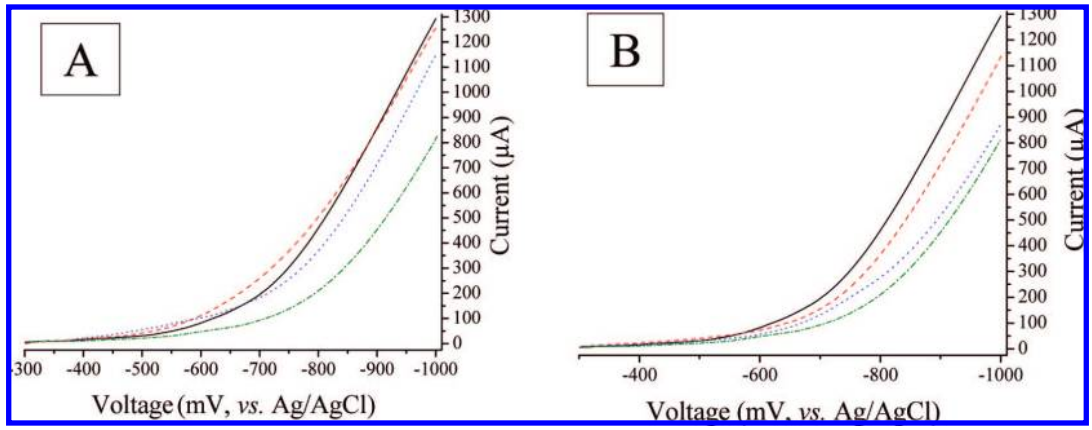

Figure 5. Current−voltage data for functionalized and unfunctionalized TiO_2 thin films in 0.5 M LiI and 0.05 M I_2: (A) Comparative data for undecanoic acid/TiO_2 (− − −), decyltriethoxysilane/TiO_2 (− • −), decylphosphonate/TiO_2 (• • •), and an unfunctionalized TiO_2 film (−); and (B) Comparative data for decyltriethoxysilane/TiO_2 (− • −), octyltriethoxysilane/TiO_2 (• • •), and hexyltriethoxysilane/TiO_2 (− − −), and an unfunctionalized TiO_2 film (−).

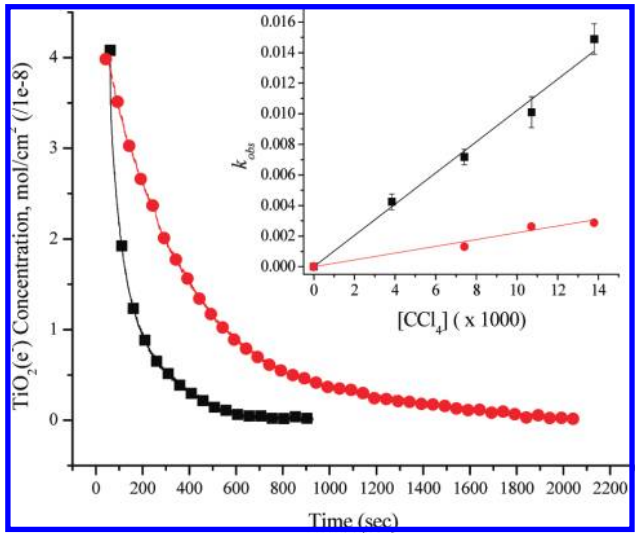

Figure 6. Concentration of $TiO_2(e^-)$ in the presence of 44 mM carbon tetrachloride for an unfunctionalized TiO_2 film (− □ −) and a decyltriethoxysilane film/TiO_2 (− ● −) as a function of time. The inset shows the dependence of observed rate (k_{obs}) on the carbon tetrachloride concentration.

in aqueous electrolytes.[2] Interestingly, however, the direction of change is opposite to that recently reported for 4-guaniodinobutyric acid/TiO_2 in ionic liquids.[14]

With Li^+ containing electrolytes, the DOS at potentials greater than ~ −400 mV were not significantly influenced by surface functionalization. Under these conditions, there appear to be some deep trap states that the surface chemistry could not eliminate. The states are likely to be related to the presence of the Li^+ cations as they occur at much more positive potentials than any electronic states observed spectroscopically in the TBA^+ electrolytes.[15] At more negative potentials the DOS for functionalized TiO_2 was clearly smaller, behavior that is reasonably attributed to decreased Li^+ adsorption. The DOS was about a factor of 2 smaller for decyltriethoxysilane/TiO_2 than unfunctionalized TiO_2, for example.

Does the electrochemical population of unfilled states in itself influence the DOS? It would be convenient if one could fill (and unfill) electronic states in the semiconductor without in turn altering the remaining DOS, but this may not be the case. Indeed with the known potential dependent adsorption and/or intercalation of cations to anatase TiO_2, the material itself is expected to change as the Fermi energy is raised.[30,34,35] In an attempt to probe this question, the excited-state injection yield of surface functionalized $Ru(dcb)(bpy)_2^{2+}$/TiO_2 thin films was quantified. An advantage of this approach is that the photon energy can be used to probe the DOS at open circuit since the quantum yield will depend on the overlap of the excited sensitizer with the acceptor states in the semiconductor.[36] A limitation in the present study is that only discrete energy levels can be probed. Here we find that there is a sufficient DOS for quantitative excited-state injection after all surface functionalizations. The reduction potentials of the Franck−Condon and thermally equilibrated excited states of $Ru(dcb)(bpy)_2^{2+}$ are −990 and −720 mV, respectively.[16] The DOS analysis shown in Figure 7 implies a high density of acceptor states at these energies. Therefore, the sensitized injection yield measurements are qualitatively in agreement with the DOS analysis.

Reactivity of Functionalized TiO_2 with Electron Acceptors. Redox inactive organic molecules have been used as "blocking layers" to enhance solar conversion efficiencies in dye-sensitized solar cells (DSSC). The remarkable enhancement of V_{oc} observed after the addition of 4-*tert*-butylpyridine to the electrolyte was attributed to 5.5×10^4-fold decrease in the rate constant for tri-iodide reduction by $TiO_2(e^-)$s.[4] For regenerative solar cells, the following relation is often used to rationalize such interfacial behavior:

$$V_{oc} = \left(\frac{\alpha kT}{e}\right)\ln\left(\frac{I_{inj}}{n\sum_i k_i[A]_i}\right) \quad (4)$$

where α is a nonideality factor, I_{inj} is the flux of electrons into the semiconductor, n is the concentration of TiO_2 electrons, and k_i is the rate constant for electron transfer to acceptor A_i. In dye-sensitized solar cells, the acceptors are generally thought to be iodine and/or tri-iodide. Equation 4 predicts a 59 mV increase in V_{oc} for an order of magnitude decrease in this rate constant at room temperature. Because surface functionalization is thought to block this reaction, they are often referred to as blocking layers.

The quantum yield for sensitized injection into TiO_2 was found to be near unity for all the surface functionalizations studied here. Therefore, the numerator in eq 4 appears to be independent of the surface chemistry. The increased open circuit photovoltages presumably indicate decreased rate constants for I_3^- reduction as has been previously asserted.[32] Indeed, a

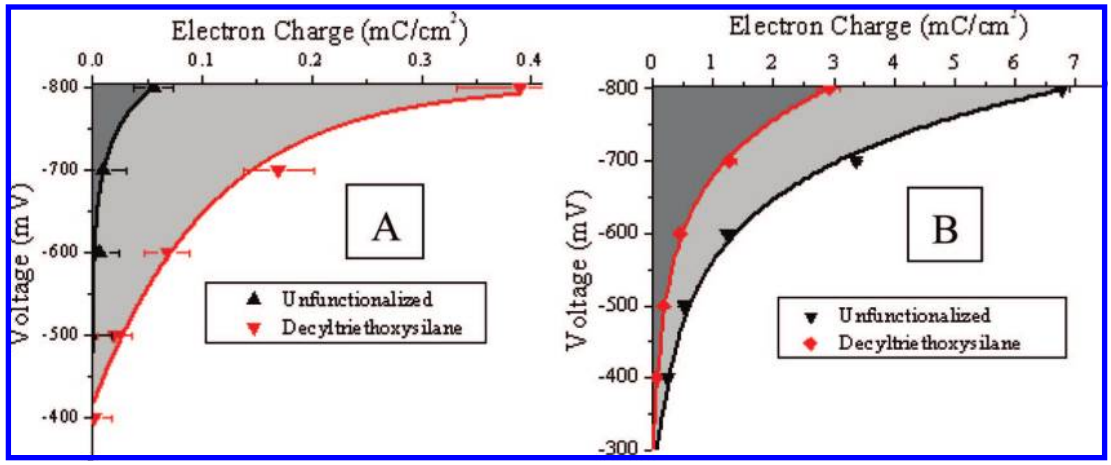

Figure 7. Electron charge assumed to correspond to the integrated density of unfilled states (DOS) of nanocrystalline anatase TiO_2 in (A) 0.1 M $TBAClO_4$ acetonitrile electrolyte and (B) 0.1 M $LiClO_4$ acetonitrile electrolyte.

7−330-fold decrease in the rate constant would be predicted by eq 4, with sensitized decyltriethoxysilane/TiO_2 showing the largest effect. This result is not new and is in agreement with previous work.[4,6−11,13,14,24,37]

A variety of other Lewis bases: 1-decylphosphonic acid, hexadecylmalonic acid, chenodeoxycholate and alkyl(trialkoxy)silanes have been utilized as blocking layers in dye sensitized solar cells.[4,6−11,13,14,24,37] In most cases enhanced energy conversion efficiencies were linked to an increase in V_{oc} through eq 4, although in some cases the current and fill factors were also influenced.[4,6−11,13,24,37] Additional insights have been gained by transient and steady state photocurrent and photovoltage measurements of operational solar cells. The magnitude of dark current observed under forward bias conditions have also been correlated with V_{oc}, an approach utilized herein.

With the exception of undecanoic acid, all surface functionalizations resulted in a decreased dark current attributed to triiodide reduction in both tetrabutylammonium and lithium containing electrolytes. In the former case, spectroelectrochemical measurements indicated a lower DOS present on the unfunctionalized TiO_2. Therefore, surface functionalization decreases the thermodynamic driving force for triiodide reduction and, although there is no direct evidence, it may inhibit I_3^- adsorption to TiO_2. Silanes appear to accomplish this more effectively than do the other functional groups. Indeed the decyltriethoxysilane/TiO_2 gave the smallest dark currents and also the highest open circuit photovoltages. To verify that surface functionalization could decrease interfacial reduction rate constants, the reactivity of $TiO_2(e^-)$s with an organohalide acceptor was quantified. The second-order rate constant for the reduction of carbon tetrachloride by decyltriethoxysilane/$TiO_2(e^-)$ was $k_{red} = 0.21 \pm 0.01\ M^{-1}\ s^{-1}$, about a factor of 5 smaller than that measured for unfunctionalized TiO_2.

Conclusions

Functionalization of mesoporous nanocrystalline (anatase) TiO_2 thin films with long chain hydrocarbons that have carboxylic acid, phosphonate, or alkoxysiloxane groups as well as hemin have been shown to have a significant influence on the density and/or reactivity of TiO_2 electrons in acetonitrile electrolytes. With tetrabutylammonium cations, surface functionalization shifts the density of states positive on an electrochemical scale (i.e., away from the vacuum level), behavior reminiscent of the effects of Bronsted acids on the flat band potential of metal oxides in aqueous environments. With Li^+ cations, surface functionalization appears to lower the overall density of states at any given potential but does not significantly influence the onset. Functionalization of the surface rendered the TiO_2 more resistant to Li^+ adsorption but did not entirely prevent it. The increased V_{oc} observed for sensitized materials was consistent with decreased rate constants for the I_3^- reduction, behavior that was directly confirmed for CCl_4 acceptors. Surface functionalization did not adversely affect excited-state injection yields. Finally, spectroelectrochemistry is a valuable tool for analysis of the TiO_2 density of states under experimentally meaningful conditions. The spectral data is not complicated by non-Faradaic processes and can be used to monitor reactivity under open circuit conditions.

Acknowledgment. This research was supported by a grant from the Division of Chemical Sciences, Office of Basic Energy Sciences, Office of Energy Research, U.S. Department of Energy (DE-FG02-96ER14662). The research on the reduction of organohalide pollutants was supported by the National Science Foundation.

Supporting Information Available: Table of IR data. This material is available free of charge via the Internet at http://pubs.acs.org.

References and Notes

(1) Vandermolen, J.; Gomes, W. P.; Cardon, F. *J. Electrochem. Soc.* **1980**, *127*, 324.
(2) Finklea, H. O.; Murray, R. W. *J. Phys. Chem.* **1979**, *83*, 353.
(3) Gomes, W. P.; Cardon, F. *Prog. Surf. Sci.* **1982**, *12*, 155.
(4) Nazeeruddin, M. K.; Kay, A.; Rodicio, I.; Humphry-Baker, R.; Mueller, E.; Liska, P.; Vlachopoulos, N.; Grätzel, M. *J. Am. Chem. Soc.* **1993**, *115*, 6382.
(5) Kusama, H.; Arakawa, H. *Sol. Energy Mater. Sol. Cells* **2004**, *81*, 87.
(6) Gregg, B. A.; Pichot, F.; Ferrere, S.; Fields, C. L. *J. Phys. Chem. B* **2001**, *105*, 1422.
(7) Kay, A.; Grätzel, M. *J. Phys. Chem.* **1993**, *97*, 6272.
(8) Huang, S. Y.; Schlichthorl, G.; Nozik, A. J.; Gratzel, M.; Frank, A. J. *J. Phys. Chem. B* **1997**, *101*, 2576.
(9) Neale, N. R.; Kopidakis, N.; vandeLagemaat, J.; Gratzel, M.; Frank, A. J. *J. Phys. Chem. B* **2005**, *109*, 23183.
(10) Hara, K.; Dan-oh, Y.; Kasada, C.; Ohga, Y.; Shinpo, A.; Suga, S.; Sayama, K.; Arakawa, H. *Langmuir* **2004**, *20*, 4205.
(11) Spivack, J.; Siclovan, O.; Gasaway, S.; Williams, E.; Yakimov, A.; Gui, J. *Sol. Energy Mater. Sol. Cells* **2006**, *90*, 1296.
(12) Wang, P.; Klein, C.; Humphy-Baker, R.; Zakeeruddin, S. M.; Grätzel, M. *Appl. Phys. Lett.* **2005**, *86*, 123508.
(13) Wang, P.; Zakeeruddin, S. M.; Humphry-Baker, R.; Moser, J. E.; Grätzel, M. *Adv. Mater.* **2003**, *15*, 2101.

(14) Zhang, Z.; Zakeeruddin, S. M.; O'Regan, B. C.; Humphry-Baker, R.; Grätzel, M. *J. Phys. Chem. B* **2005**, *109*, 21818.

(15) Redmond, G.; Fitzmaurice, D. *J. Phys. Chem.* **1993**, *97*, 1426.

(16) Kelly, C. A.; Farzad, F.; Thompson, D. W.; Stipkala, J. M.; Meyer, G. J. *Langmuir* **1999**, *15*, 7047.

(17) Fabregat-Santiago, F.; Mora-Sero, I.; Garcia-Belmonte, G.; Bisquert, J. *J. Phys. Chem. B* **2003**, *107*, 758.

(18) Heimer, T. A.; D'Arcangelis, S. T.; Farzad, F.; Stipkala, J. M.; Meyer, G. J. *Inorg. Chem.* **1996**, *35*, 5319.

(19) Bergeron, B. V.; Kelly, C. A.; Meyer, G. J. *Langmuir* **2003**, *19*, 8389.

(20) Finklea, H. O.; Vithanage, R. *J. Phys. Chem.* **1982**, *86*, 3621.

(21) Finnie, K. S.; Bartlett, J. R.; Woolfrey, J. L. *Langmuir* **1998**, *14*, 2744.

(22) Kim, C. S.; Lad, R. J.; Tripp, C. P. *Sensors Actuators B: Chem.* **2001**, *76*, 442.

(23) Kurth, D. G.; Bein, T. *Langmuir* **1995**, *11*, 578.

(24) Wang, P.; Zakeeruddin, S. M.; Comte, P.; Charvet, R.; Humphry-Baker, R.; Grätzel, M. *J. Phys. Chem. B* **2003**, *107*, 14336.

(25) Anderson, S.; Constable, E. C.; Dare-Edwards, M. P.; Goodenough, J. B.; Hamnett, A.; Seddon, K. R.; Wright, R. D. *Nature* **1979**, *280*, 571.

(26) Bookbinder, D. C.; Wrighton, M. S. *J. Electrochem. Soc.* **1983**, *130*, 1080.

(27) Moses, P. R.; Wier, L.; Murray, R. W. *Anal. Chem.* **1975**, *47*, 1882.

(28) Liu, F.; Yang, M.; Meyer, G. J. Molecule-to-Particle Charge Transfer in Sol-Gel Materials. In *Handbook of Sol-Gel Science and Technology: Processing Characterization and Application; Volume II: Characterization of Sol-Gel Materials and Products*; Almeida, R. M., Ed.; Kluwer Academic Publishers: Norwell, MA, 2005; p 400.

(29) Redmond, G.; Fitzmaurice, D.; Grätzel, M. *J. Phys. Chem.* **1993**, *97*, 6951.

(30) Rothenberger, G.; Fitzmaurice, D.; Grätzel, M. *J. Phys. Chem.* **1992**, *96*, 5983.

(31) Cao, F.; Oskam, G.; Searson, P. C.; Stipkala, J. M.; Heimer, T. A.; Farzad, F.; Meyer, G. J. *J. Phys. Chem.* **1995**, *99*, 11974.

(32) Boschloo, G.; Fitzmaurice, D. *J. Phys. Chem. B* **1999**, *103*, 7860.

(33) Kay, A.; Humphry-Baker, R.; Grätzel, M. *J. Phys. Chem.* **1994**, *98*, 952.

(34) Lyon, L. A.; Hupp, J. T. *J. Phys. Chem. B* **1999**, *103*, 4623.

(35) van de Krol, R.; Goossens, A.; Schoonman, J. *J. Phys. Chem. B* **1999**, *103*, 7151.

(36) Gerischer, H. *Pure Appl. Chem.* **1980**, *52*, 2649.

(37) He, J.; Benko, G.; Korodi, F.; Polivka, T.; Lomoth, R.; Akermark, B.; Sun, L.; Hagfeldt, A.; Sundstrom, V. *J. Am. Chem. Soc.* **2002**, *124*, 4922.

JP801338Y